Cell Biol Toxicol (2021) 37:401–419
https://doi.org/10.1007/s10565-020-09550-4

ORIGINAL ARTICLE

Elevating sestrin2 attenuates endoplasmic reticulum stress and improves functional recovery through autophagy activation after spinal cord injury

Yao Li · Jing Zhang · Kailiang Zhou · Ling Xie · Guangheng Xiang · Mingqiao Fang · Wen Han · Xiangyang Wang · Jian Xiao

Received: 21 March 2020 / Accepted: 27 July 2020 / Published online: 1 August 2020

Abstract Spinal cord injury (SCI) is a devastating neurological trauma that causes losses of motor and sensory function. Sestrin2, also known as hypoxia inducible gene 95, is emerging as a critical determinant of cell homeostasis in response to cellular stress. However, the role of sestrin2 in the neuronal response to endoplasmic reticulum (ER) stress and the potential mechanism remain undefined. In this study, we investigated the effects of sestrin2 on ER stress and delineated an underlying molecular mechanism after SCI. Here, we found that elevated sestrin2 is a protective process in neurons against chemical ER stress induced by tunicamycin (TM) or traumatic invasion, while treatment with PERK inhibitor or knockdown of ATF4 reduces sestrin2 expression upon ER stress. In addition, we demonstrated that overexpression of sestrin2 limits ER stress, promoting neuronal survival and improving functional recovery after SCI, which is associated with activation of autophagy and restoration of autophagic flux mediated by sestrin2. Moreover, we also found that sestrin2 activates autophagy dependent on the AMPK-mTOR signaling pathway. Consistently, inhibition of AMPK abrogates the effect of sestrin2 on the activation of autophagy, and blockage of autophagic flux abolishes the effect of sestrin2 on limiting ER stress and neural death. Together, our data reveal that upregulation of sestrin2 is an important resistance mechanism of neurons to ER stress and the potential role of sestrin2 as a therapeutic target for SCI.

Keywords sestrin2 · Endoplasmic reticulum stress · Autophagy · Spinal cord injury · Apoptosis

Yao Li and Jing Zhang contributed equally to this work.

Electronic supplementary material The online version of this article (https://doi.org/10.1007/s10565-020-09550-4) contains supplementary material, which is available to authorized users.

Y. Li · K. Zhou · G. Xiang · M. Fang · X. Wang (✉) · J. Xiao
Department of Orthopaedics, The Second Affiliated Hospital and Yuying Children's Hospital of Wenzhou Medical University, Wenzhou 325000 Zhejiang, China
e-mail: xiangyangwang@wmu.edu.cn

Y. Li · J. Zhang · K. Zhou · L. Xie · G. Xiang · M. Fang · W. Han · J. Xiao (✉)
Research Units of Clinical Translation of Cell Growth Factors and Diseases Research of Chinese Academy of Medical Science, School of Pharmaceutical Science, Wenzhou Medical University, Wenzhou 325000 Zhejiang, China
e-mail: xfxj2000@126.com

Y. Li · K. Zhou · G. Xiang · M. Fang
The Second School of Medicine, Wenzhou Medical University, Wenzhou 325000 Zhejiang, China

Introduction

Traumatic spinal cord injury (SCI) is a devastating central neurological disorder that leads to sensory deficits and physical disabilities and affects thousands of individuals worldwide (Badhiwala et al. 2019). The physiological progression of SCI is characterized by a series of secondary molecular events, including inflammatory response, mitochondrial dysfunction and

oxidative stress, and axonal demyelination, which cause neuronal death and injury beyond the initial mechanical damage (Silva et al. 2014).While there is yet no completely satisfactory therapy for the treatment of SCI in clinical trials, separately or combined, targeting these secondary reactions has been regarded as proper therapeutic strategies and has promoted functional recovery in most animal cases (Li et al. 2019; Ohtake et al. 2019; Wang et al. 2018a, b).

As a stress-inducible protein induced upon various stresses, sestrin2 is essential for maintaining cell metabolism and homeostasis by regulating a series of kinases and pathways, and loss of sestrin2 can result in metabolic disturbance and mitochondrial dysfunction (Lee et al. 2013; Pasha et al. 2017; Ho et al. 2016). Sestrin2 has been shown to be capable of combating oxidative stress and apoptosis by mTOR by activating AMPK. Importantly, sestrin2 was originally discovered in hypoxic conditions, and the responsive induction of sestrin2 is associated with HIF-1α stabilization (Lee et al. 2013; Olson et al. 2011). Extensive evidence has confirmed that upregulated sestrin2 protects the heart against ischemic heart injury, alleviates insulin resistance, and delays the progression of neurodegenerative diseases (Chen et al. 2014; Li et al. 2017; Morrison et al. 2015).

In addition, numerous evidence have indicated that sestrin2 provides beneficial effects in acute central nervous system injury. As a previous study reported, sestrin2 was upregulated in the cortical region in an acute stroke model in rats (Budanov et al. 2002). Further studies revealed that silencing of sestrin2 aggravates cerebral infarct but that overexpression of sestrin2 enhanced angiogenesis and attenuates focal cerebral ischemic injury under ischemic conditions, the potential mechanisms of which are related to the phosphorylation of AMPK and activation of Nrf2 (Li et al. 2016; Wang et al. 2019). Previous studies have indicated that neurons are vulnerable to the various stresses of stimulation induced by damage to the microcirculation and mechanical destruction, and maintaining neuron homeostasis is a feasible method for functional recovery (Courtine and Sofroniew 2019; Tator and Fehlings 1991). Based on the versatile function of sestrin2 exhibited above, we hypothesized that sestrin2 is highly advantageous to neuronal homeostasis in the spinal cord. However, the role of sestrin2 in neuronal response to traumatic SCI has not been well elucidated.

The endoplasmic reticulum (ER) serves the major site for protein synthesis and controls the quality of newly synthesized proteins (Borgese et al. 2006). The perturbation of ER environment homeostasis leads to the overabundance of misfolded proteins and ER stress (Araki and Nagata 2011; Yin et al. 2017). Though the unfolded protein response (UPR) can attenuate misfolded proteins, durative ER stress without treatment ultimately exceeds the compensation and turns UPR into a pro-death pathway (Valenzuela et al. 2012; Morris et al. 2018). Accordingly, maintaining ER homeostasis is vital for neuron regeneration and function (Wan et al. 2019; Zhao et al. 2016). In particular, a study (Park et al. 2014) showed that ER stress suppressed by sestrin2 is important for hepatic rehabilitation. Therefore, we reasoned that sestrin2 plays a critical role in regulating neural ER stress. Considerable evidence has indicated a link between UPR and autophagy, in which the initiation of ER stress often stimulates the autophagic activity and autophagy acts as a compensatory protection for eliminating aggregated misfolded proteins (Cai et al. 2016; Liu et al. 2015; Nakka et al. 2016). Meanwhile, it has been found that sestrin2 can activate autophagy under various pathological stresses, and deficiency of sestrin2 results in an impairment of autophagy (Ho et al. 2016; Lee et al. 2010). As described previously, ER stress limited by sestrin2 may be related to the activation of autophagy. However, the relationship of sestrin2, autophagy, and ER stress in neural injury remains elusive.

Given that sestrin2 performs such critical and versatile physiological functions and prevents the progression of diverse pathologies, we sought to define the role of sestrin2 in ER stress and autophagy in neurons and the therapeutic effect on SCI. In the current study, we hypothesized that ER stress is involved in sestrin2 regulation and that induction of sestrin2 would activate autophagy, enhance ER homeostasis and reduce neuronal apoptosis in a mouse model of acute SCI, decreasing the size of the damage and enhancing neural regeneration and functional recovery.

Materials and methods

Reagents and antibodies

TBHP (#416665) was purchased from Sigma-Aldrich (WI, USA), and GSK2606414 (#HY-18072), KIRA6 (#HY-19708), Baf-A1 (#HY-100558), TM (#HY-A0098), CQ (#HY-17589A), and Compound C (#HY-

13418A) were purchased from MCE (NJ, USA) and dissolved in DMSO (Solarbio, #D8371, Beijing, China). NGF was purchased from Sino Biological (#11050-HNAC, Beijing, China). RPMI1640 medium (#21870076), penicillin/streptomycin solution (#15140122), neurobasal medium (#21103049), and B27 Supplement (#17504044) were purchased from Gibco (CA, USA). Fetal bovine serum (#p30–3301) was purchased from PAN-Biotech GmbH (Baghlia, Germany). Bovine serum albumin was purchased from Sigma (#A7030, Shanghai, China). The related information of primary antibodies used in the study is listed in Supplemental Table 1. Alexa Fluor 488-labeled and Alexa Fluor 647-labeled goat anti-rabbit/mouse/rat secondary antibodies were purchased from Abcam (MA, USA). 4, 6-Diami-dino-2-phenylindole (DAPI) was obtained from Beyotime (#P0131, Shanghai, China).

Mouse spinal cord injury model

Briefly, adult mice were anesthetized with 4% (*w*/*v*) chloral hydrate (3.5 mL/kg, i.p.), and a laminectomy was performed at the T9 level after incision of skin and muscle adjacent to the spinous processes. For the SCI group, the exposed spinal cord was subjected to a moderate crush injury through a 10 g weight from a height of 20 mm (Zheng et al. 2019). After muscle and skin were sutured, mice received 0.5 mL of normal saline and were returned to a warm blanket for postoperative recovery. For the control group, a laminectomy was performed without crush injury.

Drug administration

To induce chemical ER stress in the spinal cords of mice, TM solution (1 mg/kg/day) was applied to mice by intraperitoneal injection for 2 days (Salvany et al. 2019). To inhibit lysosomal function, bafilomycin-A1 (0.3 mg/kg) was injected intraperitoneally daily from the seventh day after AAV injection to end of transfection (Zheng et al. 2019). Chloroquine (50 mg/kg) was administered intraperitoneally daily starting from 3 days before SCI and continued until the mice were euthanized (Zhang et al. 2017). Compound C (10 mg/kg/day, i.p.) was applied to mice from the seventh day after AAV injection to the end of transfection (Yu et al. 2008).

AAV intrathecal injection

AAV vectors containing the genes for sestrin2 (#230784) and empty vectors were constructed by GeneChem (#GOSV0196538, Shanghai, China). Virus delivery by intrathecal injection was performed in adult mice using a method as described previously (Parikh et al. 2011). Following anesthesia with chloral hydrate by intraperitoneal injection, the lamina of the L5 and L6 region was exposed, and a small laminectomy was made for exposure of the spinal dura mater. AAV particles at 5×10^{12} were injected in 2 μl of viral solution per site using a 10-μL Hamilton syringe with a 32-gauge needle at a rate of 0.2 μl/min. After injection and suture were completed, mice were placed on a warm blanket for postoperative recovery. No mice exhibited hind limb paralysis or paresis after injection.

Animal groups

All protocols and animal experiments were conducted in strict accordance with the Animal Care and Use Committee of Wenzhou Medical University (No. wydw-2018–0043). A total of 256 adult female C57BL/6 mice (7 to 8 weeks old, 20–25 g) were obtained from Wenzhou Medical University; 240 mice survived and were divided into 13 groups: a control group ($n = 27$), an SCI group ($n = 39$), an AAV-control group ($n = 22$), an AAV-control + SCI group ($n = 34$), an AAV-sestrin2 group (n = 22), an AAV-sestrin2 + SCI group ($n = 37$), an AAV-control + Baf-A1 group ($n = 6$), an AAV-sestrin2 + Baf-A1 group (n = 6), an AAV-sestrin2 + CQ group ($n = 12$), an AAV-sestrin2 + SCI + CQ group (n = 12), an AAV-sestrin2 + Compound C group ($n = 9$), a TM group (n = 9), and a pregnant group ($n = 5$).

Cell culture and drug administration

PC12 cells, a cell line derived from rat pheochromocytoma, were obtained from the Cell Storage Center of Wuhan University (Wuhan, China) and differentiated into neuron-like morphology by NGF (50 ng/mL) treatment for 3 days before any drug intervention. PC12 cells were cultured in RPMI1640 medium with 10% fetal bovine serum and 1% antibiotic-antimycotic at 37 °C with 5% CO_2. Primary cortical neurons were obtained from 21 postnatal Day 0 (P0) mouse pups by dissecting the cerebral cortex as described previously (Li et al. 2019). Neurons were

seeded on a poly-D-lysine-coated 12-well plate at a density of 3–5 × 10^5 cells per well and incubated in neurobasal medium supplemented with 2% B27 Supplement (neuronal cell culture supplement) at 37 °C in a humidified 5% CO_2-containing atmosphere. Half of the culture media was replaced with fresh on day 2 and every 3 days, and neurons were cultured for an additional seven days before use. For injury stimulation and chemical ER stress in vitro, cells were respectively treated with TBHP (50 μM) and TM (2 μg/mL) in a time-dependent manner as designed.

siRNA transfection

The siRNA targeting mouse ATF4 and ATF6 and negative control siRNA were obtained from GenePharma (A10001; Shanghai, China). Cultured PC12 cells were transfected following the manufacturer's instructions. In brief, cells were seeded on a 6-well plate and cultured to 60% confluence and reverse transfected with 25 nM negative control or siRNA duplexes using Lipofectamine 2000 siRNA transfection reagent (#11668019, Thermo Fisher Scientific, MA, USA). After 48 h of incubation, cells were treated with TM (2 μg/mL) for 12 h.

Behavior assessment

BMS. The BMS score was used to evaluate the hindlimb motor function on the coordination in movement at the following time points: baseline, 2, 7, 14, 21, 28, 35, and 42 days after injury (Basso et al. 2006). The mice were placed in an open field and allowed to move freely for 5 min and observed for a period of 2 min. The average of the scores was measured when the scores of the right and left hindlimbs were different.

Balance beam test The balance beam test was used to assess the motor coordination and balance during walking on a beam with slight modification from a previous report (Doeppner et al. 2014). The beam is 110 cm long with gradually reduced width and is suspended 15 cm from the ground. The width of the beam is 12 mm at the beginning and 5 mm at the end, with a platform. The measurement of the test is the time in which mice reach the platform from the beginning. The maximum allowable walking time is 60 s; the time is recorded as 60 s if the mice fail to reach the destination.

Inclined plane test The inclined plane test was performed for evaluation of the strength of hindlimbs, as described previously (Li et al. 2019). In brief, the mice were put on a board with a rubber surface. With a continuous increase of the board angle, the maximum angle was recorded and defined as the value at which the mouse could not maintain its position for 5 s without falling. Each mouse was assessed in three trials and given 1 min for a break.

Tissue preparation

Mice were euthanized at specific time points, and ventricular perfusion was performed with phosphate-buffered saline (PBS). A 10-mm-long spinal cord sample centered around the contusion epicenter was obtained and stored at −80 °C immediately for the preparation of western blotting. For staining, mice were perfused with PBS and 4% paraformaldehyde (PFA), and spinal cord samples from 10-mm longitudinal sections centered around the lesion epicenter were dissected out, post fixed in 4% PFA for 6 h, and embedded in paraffin before being cut into 0.5-μm slices.

Western blot assay

For in vivo analysis, 5-mm tissue samples of spinal cord from around the injury center were collected from SCI mice or the same area of control mice. Cell lysates were prepared by lysing the PC12 cells in 6-well plates. Proteins were quantified using BCA reagents (#23225, Thermo Fisher, MA, USA), and equivalent amounts of protein (80 μg in vivo, 40 μg in vitro) were separated on SDS-PAGE gels and transferred to polyvinylidene fluoride (PVDF) membranes (#1620256, Bio-Rad, CA, USA). Membranes were blocked with 5% nonfat milk in TBST (Tris-buffered saline with 0.1% Tween-20) and then incubated overnight at 4 °C with primary antibodies. The titers of primary antibodies are listed in Supplemental Table 1. The membranes were washed with TBST and incubated with secondary antibodies for 90 min at room temperature. Protein bands were detected using a ChemiDoc XRS + Imaging System (Bio-Rad, CA, USA), and the bands were quantified using densitometric measurement by Quantity-One software (Version 4.6.9).

Immunofluorescence staining

Longitudinal and transverse sections of 5-μm thickness were cut, deparaffinized, rehydrated, and washed in PBS. Primary cortical neurons were seeded on coverslips in 12-well plates, fixed for 15 min in 4% PFA, and washed in PBS three times for 2 min each. The sections were then incubated with 5% bovine serum albumin for 30 min and then incubated with the primary antibodies overnight at 4 °C in the same buffer. The titers of primary antibodies are listed in Supplemental Table 1. After primary antibody incubation, sections were washed and then incubated in secondary antibodies for 60 min at 37 °C. Sections were rinsed in PBS, labeled with DAPI for 7 min, and sealed with a coverslip. Images were observed using a Nikon ECLIPSE Ti microscope (Nikon, Tokyo, Japan) and analyzed by ImageJ (Version 1.52p).

TUNEL staining

A TUNEL assay was performed according to the manufacturer's instructions (#40307ES60, Yeasen Biochemical, Shanghai, China). Briefly, sections were cut from the areas 4–5 mm rostral and caudal from the contusion center of the mouse spinal cord tissue, incubated in 0.1% Triton X-100 for 30 min and incubated with 50 μL of TUNEL reaction mixture. Finally, the sections were stained with DAPI and observed using a Nikon ECLIPSE Ti microscope.

Statistical analysis

Data are presented as the mean ± standard deviation (SD). Statistical analyses were performed using GraphPad Prism (Version 8.0.2). Parametric data (normality and equal variance passed) were analyzed using one-way analysis of variance (ANOVA) followed by Dunnett's test for between-group comparisons. Equal variance failed data were analyzed using Kruskal-Wallis ANOVA based on ranks followed by Dunn's post hoc test. Comparisons at multiple time points were analyzed with a repeated measures ANOVA followed by an LSD test for between-group comparisons. The results of only two groups were analyzed using the unpaired student *t* test for equal variance passed data and the Mann-Whitney rank-sum test for equal variance failed data. A P value < 0.05 was considered significant.

Results

Expression of sestrin2 after spinal cord injury

To determine expression changes in sestrin2 in mouse neurons after SCI, we evaluated the expression levels of this protein in a time-dependent manner by western blot and immunostaining. First, no obvious differences in sestrin2 expression were found at the different time points in intact mice by both western blot (Figs. S1a–c) and immunostaining (Figs. S1d–e). Compared with the control group, sestrin2 protein levels were increased at days 1 and 3 after injury and decreased at days 7 and 14 after injury (Fig. 1a–b). In addition, the immunofluorescence staining result also indicated that sestrin2 was mainly expressed in neurons (Fig. 1c–d). Furthermore, the sestrin2 expression in PC12 cells was evaluated when cells were subjected to TBHP stimulation. The results of western blot showed that sestrin2 expression was increased in response to TBHP insult (Figs. 1e–f). Regarding to primary cortical neurons, the immunofluorescence staining colocalization of sestrin2 with Tuj1 indicated that treatment with TBHP manner enhanced sestrin2 expression in a time-dependent (Fig. 1g–h). Overall, these data suggested that sestrin2 is upregulated after SCI and may provide a protective effect in response to neural injury.

ER stress increases sestrin2 expression

ER stress is a series of processes characterized by the perturbation in ER homeostasis with misfolded/unfolded protein accumulation, which is extensively present in SCI and aggravates neural injury (Yin et al. 2017). We reasoned that ER stress may relate to the sestrin2 induction and first monitored the expression level of sestrin2 with the treatment of chemical ER stress inducers in vivo. GRP78 and PDI are recognized as ER chaperones, and their levels increase when misfolded proteins accumulate. The results indicated that tunicamycin (TM) treatment significantly increased the expression of GRP78, PDI, CHOP, and sestrin2 in the

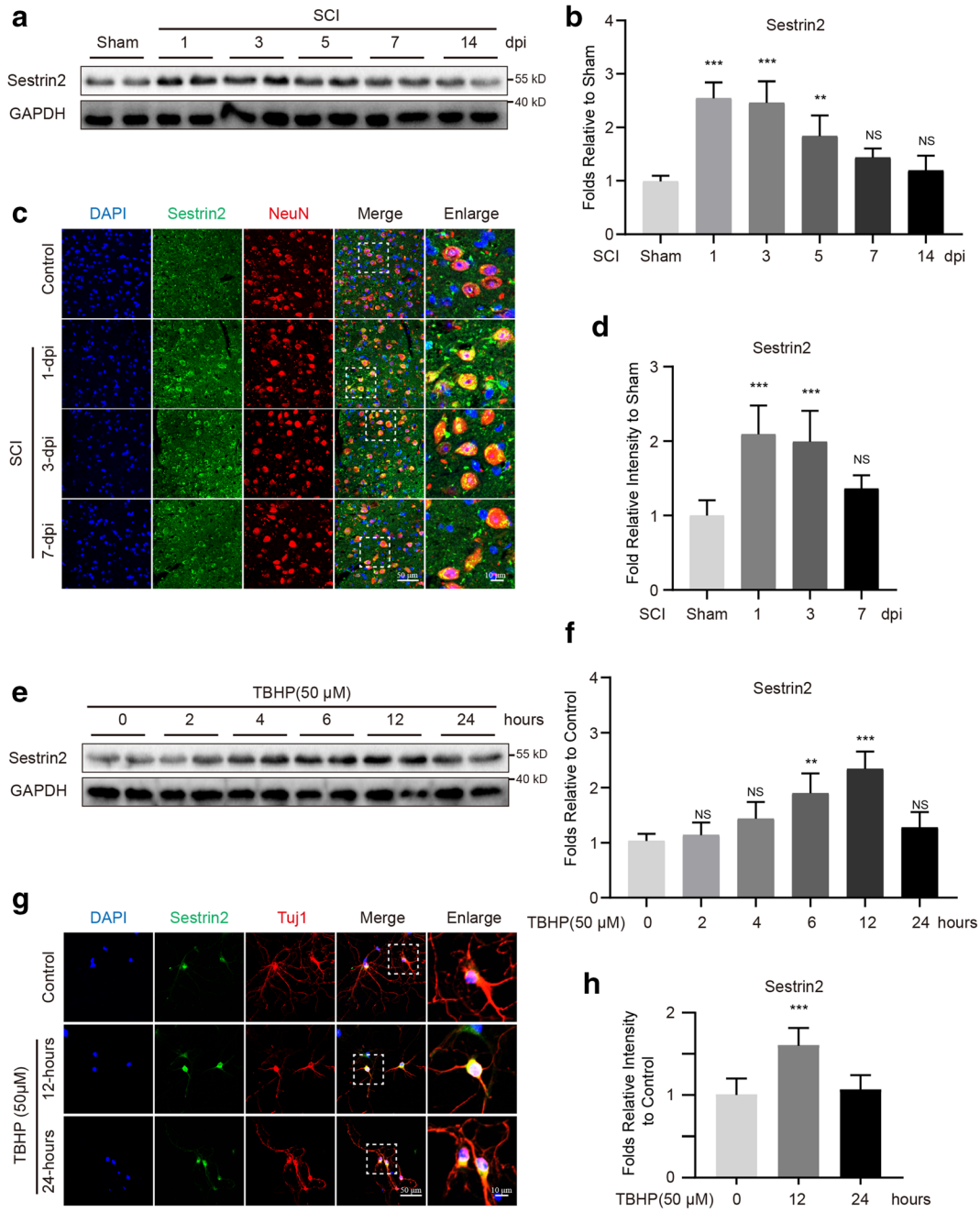

Fig. 1 Injury stimulation induces sestrin2 upregulation in vivo and vitro. (**a** and **b**) Western blot and quantification of the time-dependent expression level of sestrin2 in spinal cord of mice after SCI. (**c** and **d**) Immunofluorescence of sestrin2 puncta in neuron and quantitative analysis of sestrin2 intensity in mice at different time points after SCI. Scale bar = 50 μm; scale bar (enlarged) = 10 μm. (**e** and **f**) The protein expression of sestrin2 in PC12 cells subjected to TBHP (50 μM) in a time-dependent manner. (**g** and **h**) Immunofluorescence of sestrin2 in primary cortical neurons treated with TBHP (50 μM) for 12 and 24 h. Scale bar = 50 μm; scale bar (enlarged) = 10 μm. GAPDH was the loading control. Data represent mean ± S.D. ($n = 6$). $^{*}P < 0.05$, $^{**}P < 0.01$, $^{***}P < 0.001$, NS, not significant

spinal cord compared with the control condition (Figs. S2a–b). Immunofluorescence staining also indicated that sestrin2 associated with higher intensity and mainly colocalized with NeuN in the TM treatment group (Fig.

S2c–d). In vitro, primary cortical neurons treated with TM presented an increased intensity of sestrin2 and infirm morpha (Fig. S2e–f). Thus, these results demonstrated that ER stress could induce sestrin2 expression in vivo and in vitro.

Sestrin2 induced by TM depends on the PERK-ATF4 axis

UPR is a well-known adaptive mechanism for cells against ER stress in the early stage (Valenzuela et al. 2012). To determine whether the unfolded protein response is responsible for sestrin2 induction, we determined the contribution of three transmembrane ER stress sensor proteins in vitro. As the results of western blot indicated, sestrin2 expression was markedly downregulated by pretreatment with 1 μM PERK inhibitor (GSK2606414) for 1 h, especially in PC12 cells subsequently treated with TM for 6 h (Fig. S3a–b). In contrast, inhibition of IRE1α and ATF6 was not involved in sestrin2 expression in both the control and TM treatment circumstances (Fig. S3c–f). In addition, as a well-established downstream transcription factor of PERK (Han et al. 2013), ATF4 knockdown using small interfering RNA (siRNA) resulted in a significant reduction of sestrin2 expression compared to PC12 cells transfected with NC siRNA (Fig. S3g–h). To gain further insights into the mechanism ofsestrin2 induction upon ER stress, we utilized PERK inhibitor for treating primary cortical neurons. The results of immunofluorescence staining in primary cortical neurons showed that PERK inhibitor treatment resulted in lower sestrin2 expression than no inhibitor treatment (Fig. S3i–j). Collectively, these results indicated that PERK-ATF4 plays a critical role in sestrin2 induction in response to ER stress.

Sestrin2 overexpression promotes functional recovery after SCI

To evaluate the role of sestrin2 in the spinal cord after injury, we utilized adeno-associated viral (AAV) vectors for overexpression of sestrin2 in vivo. Introduction of an AAV construct expressing sestrin2 resulted in a significantly increased sestrin2 protein level in the spinal cord (Fig. 2a–d). To evaluate the effect of sestrin2 on tissue rehabilitation, we examined the lesion volume of the spinal cord after injury. The spinal cord lesion volume was smaller in the AAV-sestrin2-treated mice in comparison with the mice that received the vehicle (Fig. 2e–f). Furthermore, to determine whether sestrin2 contributes to functional recovery in SCI mice, 6 weeks of behavioral tests, including basso mouse scale (BMS), balance beam, and inclined plane test, were performed in a blinded manner (Fig. 2g–l). As the results showed, all mice presented similar severities of injury at 2 days after SCI and progressive recovery at several weeks after SCI. It should be noted that mice that received AAV-sestrin2 displayed better functional recovery and coordination improvement than mice treated with AAV-control after SCI, especially in the later stages of injury. Specifically, the results of BMS indicated that the SCI mice treated with AAV-sestrin2 achieved higher scores than mice treated with vehicle AAV starting from 4 weeks after injury (Fig. 2g–h). Moreover, assessments of balance beam (Fig. 2i–j) and inclined plane test (Fig. 2k–l) suggested that SCI mice injected with AAV-sestrin2 performed better in motor coordination, balance, and strength of hindlimbs in comparison to corresponding injury controls from 3 to 6 weeks. These results demonstrated that upregulation of sestrin2 is responsible for functional recovery after SCI.

Sestrin2 overexpression maintains ER homeostasis after SCI

Several lines of evidence have indicated that adaptive sestrin2 induction protects cells against ER stress (Park et al. 2014; Pasha et al. 2017). Using western blot assay, sestrin2 overexpression was determined to be sufficient to reduce the expression of GRP78 and PDI compared with empty vectors after SCI (Fig. 3a–b). Meanwhile, sestrin2 overexpression also attenuated the expression of ubiquitinated proteins, which is a group of polypeptides that label misfolded proteins (Fig. 3c–d). Thus, sestrin2 plays a critical role in alleviating ER stress after SCI. Meanwhile, sestrin2 overexpression decreased the levels of CHOP and caspase12, which are regarded as downstream transcription factors in the execution of ER stress-induced apoptosis (Fig. 3a–b). In line with this notion, immunofluorescence staining showed that the effect of sestrin2 on reducing GRP78 (Fig. 3e–f) and CHOP (Fig. 3g–h) mainly occurred in neurons. Taken together, these results suggested that sestrin2 maintains

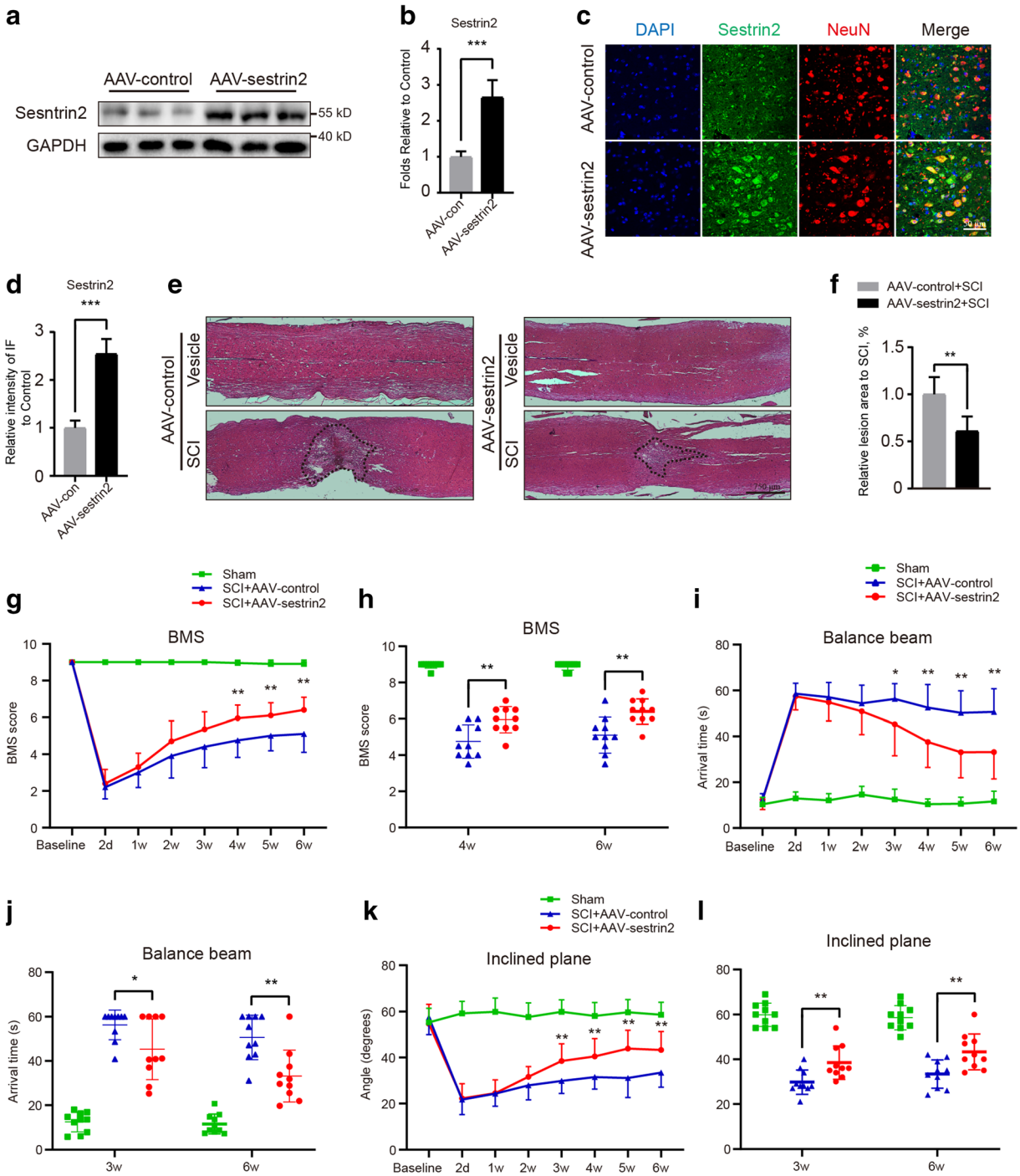

Fig. 2 Sestrin2 improves functional recovery after SCI. (**a**–**d**) Western blot and immunofluorescence of sestrin2 in spinal cord of mice after injected with AAV-control or AAV-sestrin2 for 14 days. (**e**) Representative images from H&E staining at 28 days post-injury, scale bar = 750 μm. (**f**) Quantification of the lesion area of the spinal cord from H&E staining. (**g** and **h**) Graphs of the score of BMS at different time points after SCI in mice treated with or without AAV-sestrin2 injection. (**i** and **j**) Graphs of arrival time of balance beam at different time points after SCI in mice treated with or without AAV-sestrin2 injection. (**k** and **l**) Graphs of angle of inclined plane test at different time points after SCI in mice treated with or without AAV-sestrin2 injection. GAPDH was the loading control. $^{*}P < 0.05$, $^{**}P < 0.01$, $^{***}P < 0.001$

ER homeostasis and promotes recovery from ER stress in neurons.

Sestrin2 protects neurons from apoptotic death

Prolonged ER stress eventually overruns the compensatory capacity of the ER lumen for misfolded protein aggregation and switches ER stress to a pro-death process (Engel et al. 2013). Since sestrin2 is beneficial to ER homeostasis, here we focused on examination of the functional importance of sestrin2 in neural death. Remarkably, administration of AAV-sestrin2 reduced Bax and cleaved caspase3 and increases Bcl2 expression (Fig. 4a–b) and also significantly decreased the number of TUNEL-positive cells in spinal cord (Fig. 4c–d). Consistently, immunofluorescence staining colocalization of NeuN and cleaved caspase3 were essentially in agreement with the results of western blot (Fig. 4e–f). Thus, the above data demonstrated that sestrin2 is a beneficial factor for protecting neurons from apoptosis.

Sestrin2 activates autophagy in the spinal cord

Despite evidence identifying sestrin2 as a regulator of the autophagy lysosome pathway, its function in neurons is still unclear and was examined here (Ho et al. 2016; Li et al. 2017). Western blot showed that overexpression of sestrin2 in the spinal cords of mice markedly upregulated the levels of p62, LC3-II/I, CTSB, and Lamp2,which are corresponding proteins regulating autophagosome formation and lysosomal biogenesis (Fig. 5a–b). Meanwhile, higher intensities of LC3 (Fig. 5c–d) and Lamp2 (Fig. 5e–f) were detected in neurons with sestrin2 overexpression. Considering that autophagy is a dynamic process and that the LC3-II level may decrease followed by autolysosomes degeneration, the expression level of LC3-II in mice intraperitoneally treated with bafilomycin-A1 (Baf-A1, 0.3 kg/mg) was proposed to quantize the gross product. The results showed that the lysosomal inhibitor successfully caused the accumulation of LC3-II, and the AAV-sestrin2 group treated with bafilomycin-A1 was associated with a higher level of LC3-II (Fig. 5g–h). Thus, autophagy activity was increased following sestrin2 upregulation.

Sestrin2 ameliorates the autophagic flux dysfunction after SCI

We investigated whether sestrin2 affects autophagic flux after SCI. There was no significant change of LC3 II/I, CTSB, and p62 at the different time points of control mice (Fig. S1a–c). Subsequently, we found significant increases in p62 and LC3-II expression and decreases in CTSB and Lamp2 expression in the spinal cord after injury (Fig. 6a–c). These data suggested that lysosomes are damaged and that autophagosomes are abnormally accumulated. In line with the above notion, we selected the third day after injury as the time point for the following assessment. As the results presented, increased protein levels of LC3-II, CTSB, and Lamp2 and a decreased protein level of p62 were observed in sestrin2-overexpressing mice in comparison with vehicle mice after injury to the spinal cord (Fig. 6d–f). Consistently, immunofluorescence analysis also showed that the fusion of LC3 and Lamp2 was decreased in the injured group, which was reversed in the AAV-sestrin2 group after SCI (Fig. 6g–i). These assessments indicated a beneficial effect of sestrin2 during the autophagic flux restoration in mice after SCI.

Inhibition of autophagic flux abrogates sestrin2-mediated protective effects after SCI

To further evaluate the beneficial role of sestrin2 for neural survival and the association of ER homeostasis with the activation of autophagy, we intraperitoneally treated AAV-sestrin2 mice with chloroquine (CQ, 50 mg/kg), which blocks autophagic flux by alkalizing the lysosomal cavity. Following CQ treatment, an obviously increased level of ER stress was not observed in the intact AAV-sestrin2 mice, while significant upregulations of GRP78, PDI, CHOP, and ubiquitinated proteins were detected in the injured AAV-sestrin2 mice (Fig. 7a–b). Immunofluorescence staining also revealed that neurons were associated with a higher signal of GRP78 in AAV-sestrin2 mice after SCI (Fig. 7c–d). Meanwhile, the CQ treatment group exhibited markedly increased TUNEL-positive cells in the spinal cord compared with the control group (Fig. 7e–f). The results of western blot also revealed that CQ treatment did not result in significant alterations in apoptotic proteins

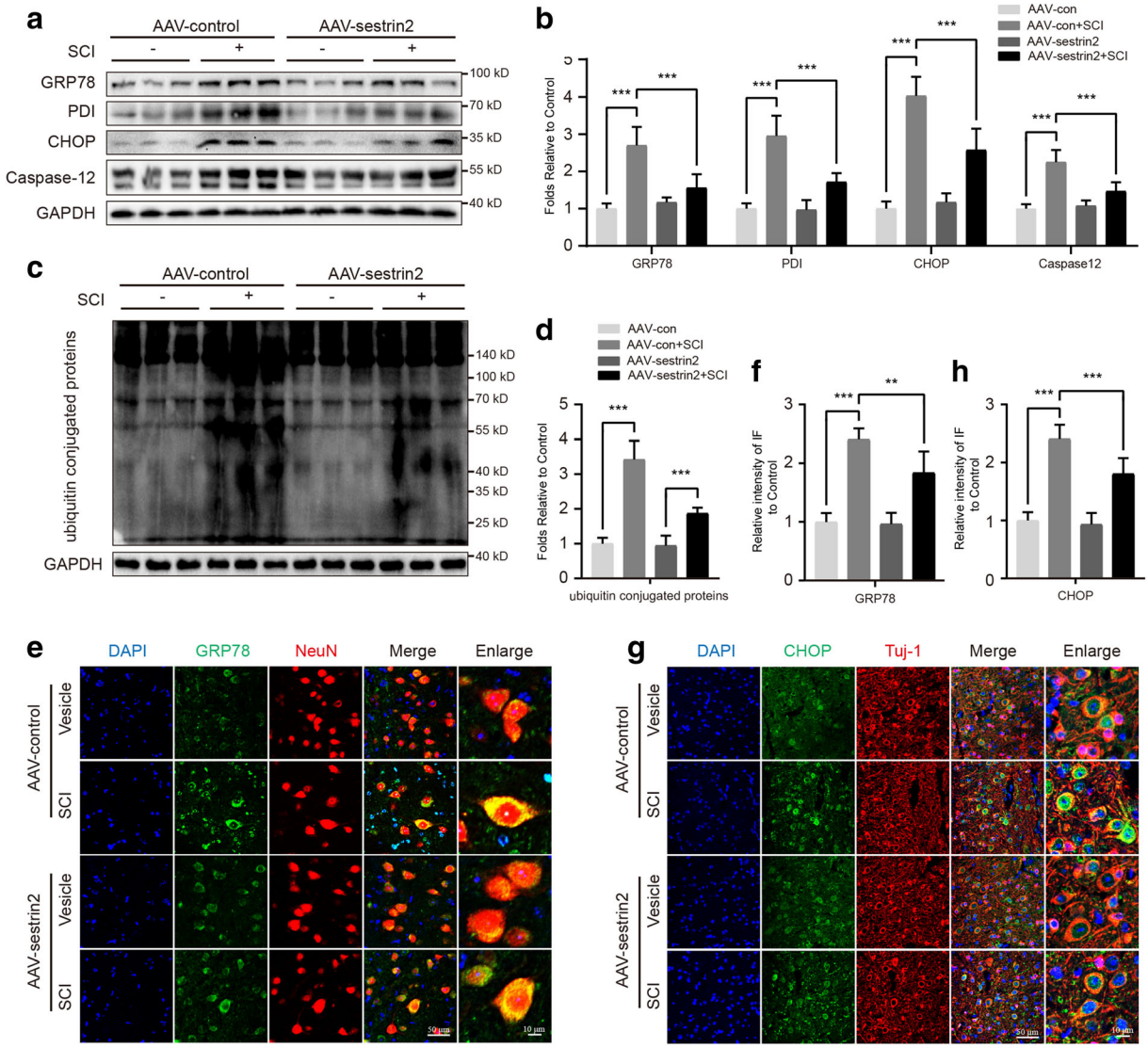

Fig. 3 Upregulation of sestrin2 contributes to ER homeostasis after SCI. (**a** and **b**) Western blot and quantification of multiple ER stress markers in spinal cord of mice in each group at 7 days after SCI. (**c** and **d**) Western blot and quantification of ubiquitin-conjugated proteins in each group at 7 days after SCI. (**e** and **f**) Double immunofluorescence of GRP78 and NeuN in sections from tissue in each group at 7 days after SCI. (**g** and **h**) Double immunofluorescence of CHOP and Tuj1 in sections from tissue in each group at 7 days after SCI. Scale bar = 50 μm; scale bar (enlarged) = 10 μm. GAPDH was the loading control. Data represent mean ± S.D. ($n = 6$). *$P < 0.05$, **$P < 0.01$, ***$P < 0.001$

in AAV-sestrin2 mice without injury, but there were marked increases in cleaved caspase3 and Bax and a decrease in Bcl-2 in AAV-sestrin2 mice with SCI (Fig. 7g–h). Therefore, these results indicated that blockage of autophagic flux by CQ treatment could significantly abolish sestrin2-induced protective effects on neural survival and ER homeostasis after SCI.

The AMPK-mTOR axis is involved in sestrin2-mediated autophagy

Since previous studies suggested that sestrin2 is involved in stress-dependent mTOR regulation, which was induced by AMPK phosphorylation, we evaluated whether sestrin2-enhanced autophagy is related to modulation of the AMPK-mTOR axis (Lee et al. 2013). As

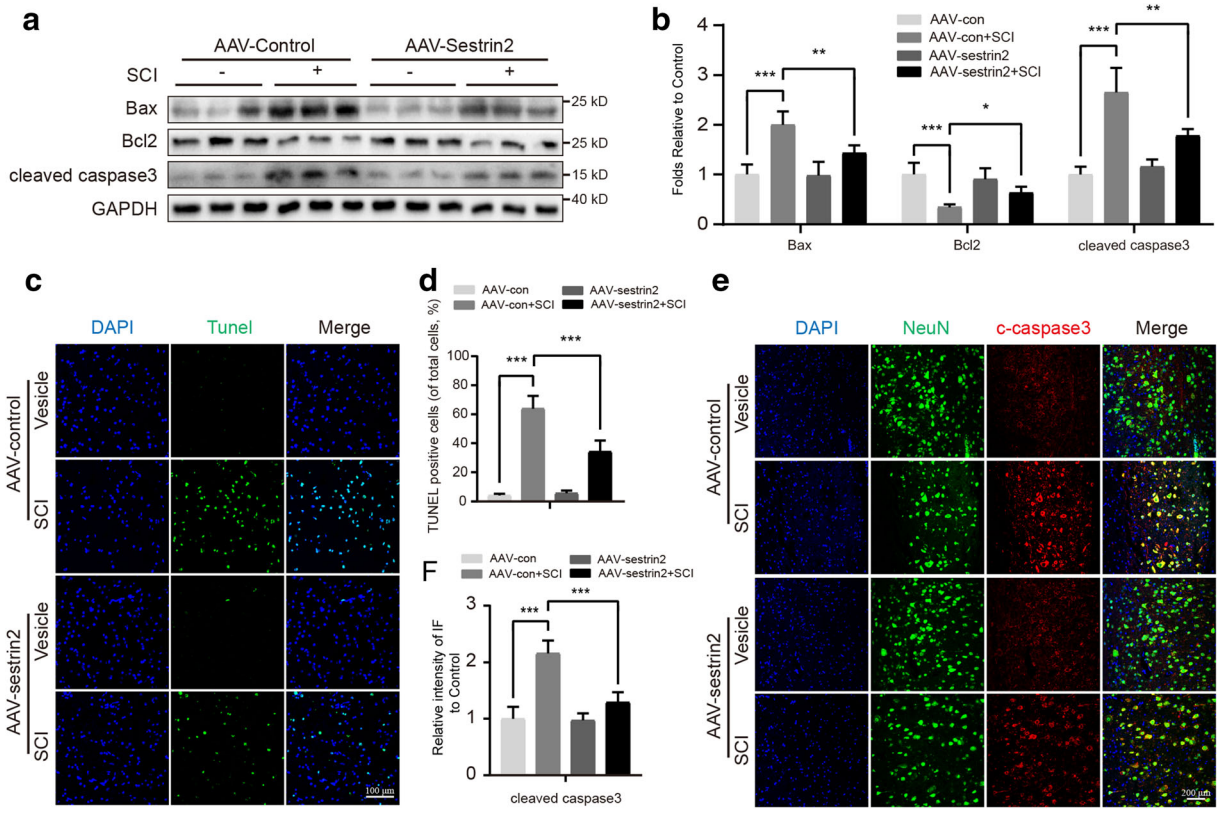

Fig. 4 Upregulation of sestrin2 reduces neural apoptosis after SCI. (**a** and **b**) Western blot and quantification of Bax, Bcl2, and cleaved caspase3 in spinal cord of mice in each group at 7 days after SCI. (**c**) Immunofluorescence staining for TUNEL (green) of sections from the spinal cord in each group 7 days after surgery, scale bar = 100 μm. (**d**) Quantitative assessment of TUNEL-positive cells from 6 independent sections from the area within 5 mm above and below the injury epicenter. (**e** and **f**) Double immunofluorescence of cleaved caspase3 and NeuN in sections from tissue in each group at 7 days after SCI, scale bar = 200 μm. GAPDH was the loading control. Data represent mean ± S.D. (n = 6). *$P < 0.05$, **$P < 0.01$, ***$P < 0.001$

the results presented (Fig. 8a–b), sestrin2 overexpression led to significant upregulation of AMPK phosphorylation and inhibition of mTOR in the spinal cord compared with the vehicle group. As a protein kinase that is responsible for the initiation of autophagy, ULK1 was also activated in AAV-sestrin2 mice. In addition, we applied Compound C to inhibit AMPK for the further assessment of the mechanism of sestrin2-induced autophagy. In mice treated with Compound C, the effect of the sestrin2-mediated increase of LC3-II and decrease of p62 was abolished (Fig. 8c–d). Consistent with the western blot data, immunofluorescence analysis revealed a lower level of LC3 in neurons of treated AAV-sestrin2 mice compared with AAV-sestrin2 vehicle mice (Fig. 8e–f). Taken together, our findings indicated that sestrin2 activated autophagy through regulation of the AMPK-mTOR signaling pathway.

Discussion

Neurons exhibit a poor capacity for intrinsic regeneration, as they have no potential for replication. Therefore, promoting neuronal survival and enhancing the surviving neuronal function are considered critical strategies for SCI therapy. This study examined the neuroprotective effect of sestrin2 in a mouse model of contusive SCI. The main result of our study is that sestrin2 is upregulated after SCI or pharmacological ER stress induced by TM treatment and that this regulation is associated with a PERK-ATF4-dependent pathway. Meanwhile, overexpression of sestrin2 contributes to maintaining ER homeostasis, limiting the damage to the spinal cord, and promoting functional recovery. The underlying mechanism for the recovery of SCI by sestrin2 is an activation of autophagy and restoration of

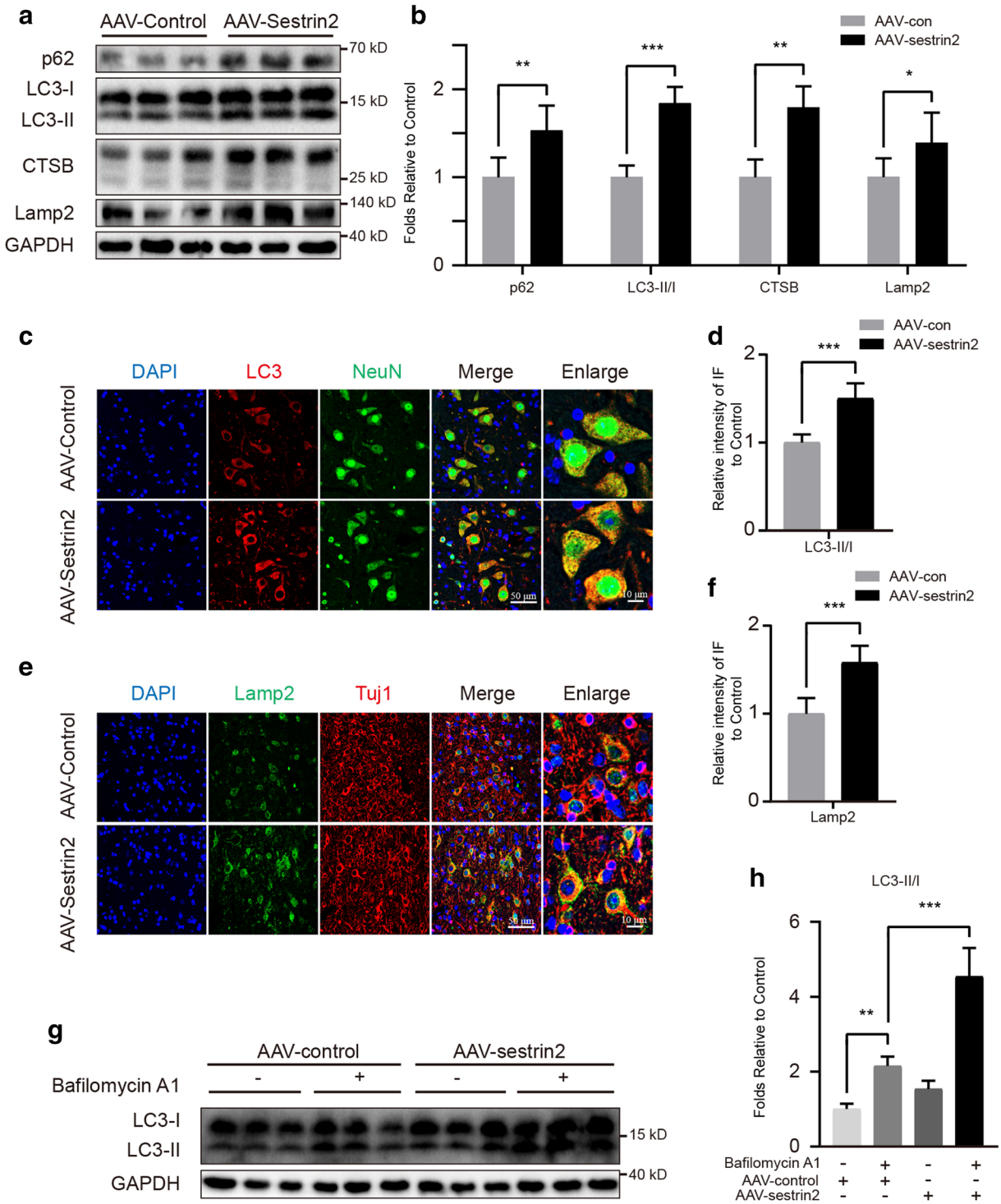

Fig. 5 Sestrin2 activates autophagy in neurons in vivo. (**a** and **b**) Western blot and quantification of p62, LC3, CTSB and Lamp2 in spinal cord of mice after injected with AAV-control or AAV-sestrin2 for 14 days. (**c** and **d**) Double staining of LC3 and NeuN in spinal cord of mice in each group, scale bar = 50 μm; scale bar (enlarged) = 10 μm. (**E** and **F**) Double staining of Lamp2 and Tuj1 in spinal cord of mice in each group, scale bar = 50 μm; scale bar (enlarged) = 10 μm. (**g** and **h**) Mice were transfected with AAV-control or AAV-sestrin2 for 14 days, and then treated with Bafilomycin A1 (0.3 mg/kg), level of LC3 was analyzed by western blot. GAPDH was the loading control. Data represent mean ± S.D. ($n = 6$). *$P < 0.05$, **$P < 0.01$, ***$P < 0.001$

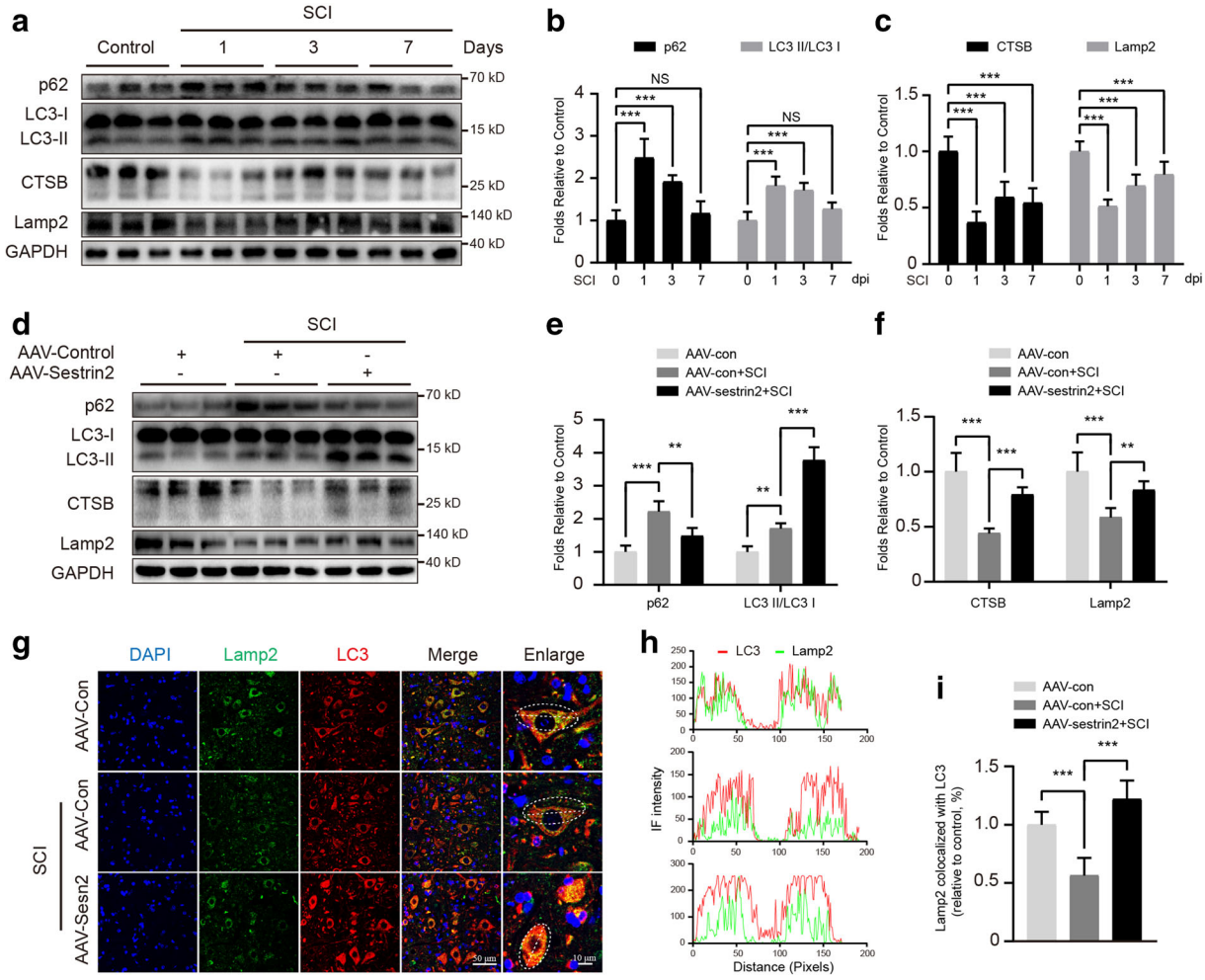

Fig. 6 Sestrin2 restores the impairment of autophagic flux after SCI. (**a**–**c**) Western blot and quantification of the time-dependent expression level of autophagy related proteins in spinal cord of mice after SCI. (**d**–**f**) Western blot and quantification of autophagy related proteins in spinal cord of mice in each group at 3 days after SCI. (**g**) Double staining of LC3 and Lamp2 in each group at 3 days after SCI. (**h**) Immunofluorescence intensity of LC3 and Lamp2 across the white dotted lines in each group, scale bar = 50 μm; scale bar (enlarged) = 10 μm. (**i**) Quantification of LC3 puncta in Lamp2 in each group. GAPDH was the loading control. Data represent mean ± S.D. ($n = 6$). $^{*}P < 0.05$, $^{**}P < 0.01$, $^{***}P < 0.001$

autophagic flux mediated by the AMPK-mTOR axis. Thus, our results suggested that manipulating sestrin2 may form a potential therapeutic strategy or become a part of combinatorial therapy for enhancing recovery after SCI.

As a highly conserved stress-inducible protein, sestrin2 appears to be a potential candidate for various pathology therapies (Ho et al. 2016; Pasha et al. 2017). A study (Morrison et al. 2015) reported that sestrin2 is a critical component in response to ischemia/reperfusion injury in the heart, and sestrin2-deficient hearts display exacerbated myocardial infarction and impaired cardiac function. Kim et al. (Kim et al. 2016) indicated that maintaining mitochondrial homeostasis and inhibiting the activation of the NLRP3 inflammasome by sestrin2 in macrophages noticeably protect the host from sepsis. Additionally, Chen et al. (2014) suggested that the induction of sestrin2 represents an endogenous protective mechanism in response to amyloid beta-peptide neurotoxicity in primary cortical neurons. More importantly, sestrin2 also provides a beneficial role in amelioration of acute ischemic brain injury (Wang et al. 2019). The results presented previously indicated that treatment with rh-sestrin2 not only reduces the disruption of the blood-brain barrier but also protects hippocampal neurons against ischemia-induced apoptosis (Shi et al.

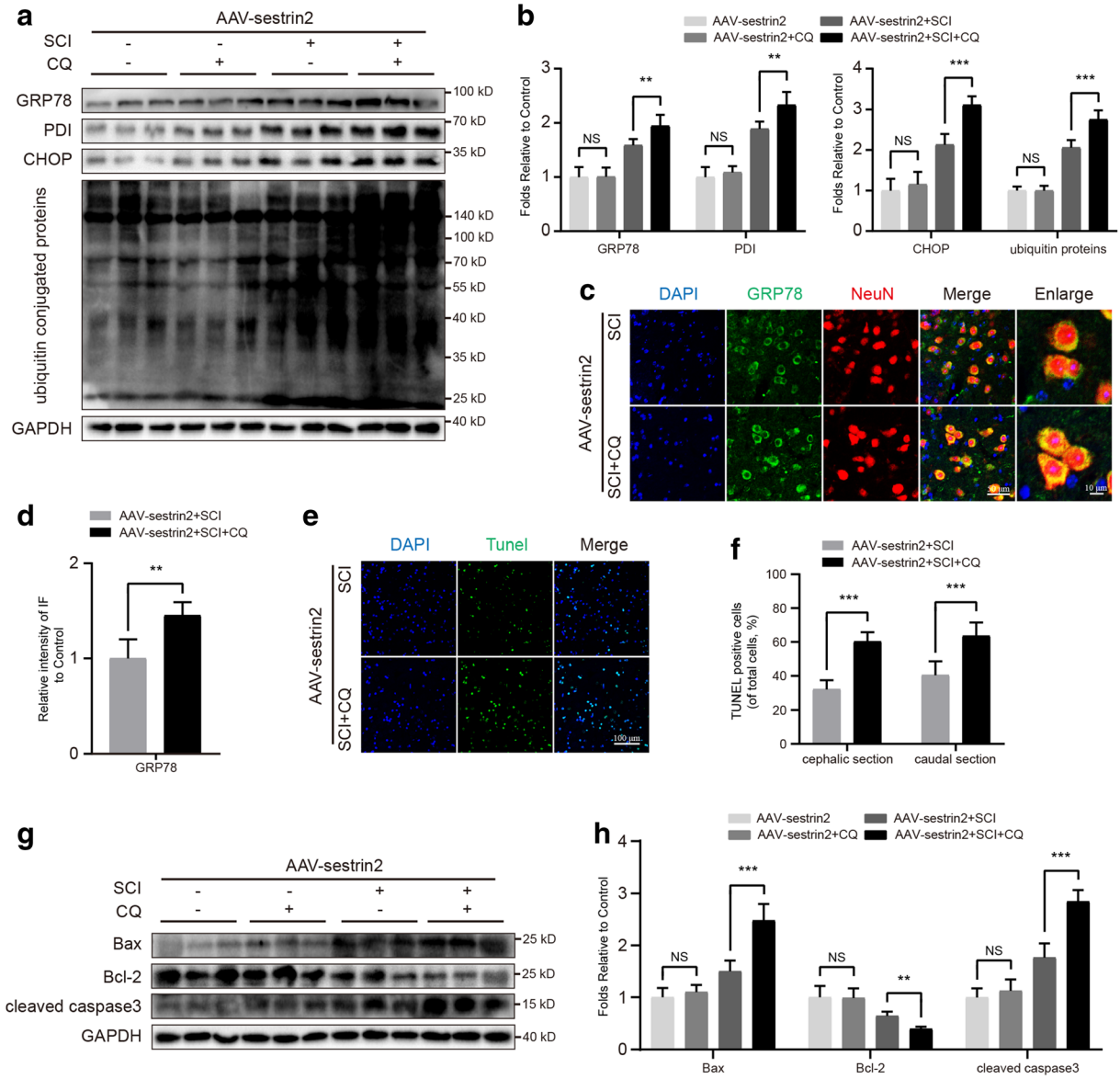

Fig. 7 Sestrin2 attenuates ER stress and apoptosis by activation of autophagy. (**a** and **b**) AAV-sestrin2 mice were pretreated with CQ (50 mg/kg) or saline at 3 days before SCI, the ER related proteins were analyzed by western blot at 3 days after SCI. (**c** and **d**) Double staining of GRP78 and NeuN in each group, scale bar = 50 μm; scale bar (enlarged) = 10 μm. (**e**) Staining for TUNEL (green) of sections from the spinal cord in each group, scale bar = 100 μm. (**f**) Quantitative assessment of TUNEL-positive cells from 6 independent sections from the area within 5 mm above and below the injury epicenter in each group. (**g** and **h**) Western blot and quantification of apoptotic proteins in each group. GAPDH was the loading control. Data represent mean ± S.D. (n = 6). *P < 0.05, **P < 0.01, ***P < 0.001

2016). Similar results were observed in the current study, as we found that overexpression of sestrin2 promotes neuronal survival and functional recovery after SCI.

The molecular mechanism of how sestrin2 provides the protective role for the above diseases is an important issue. Previous studies indicated that sestrin2 is one of the several antioxidant defenses and exhibits similar functional sequence with alkylhydroperoxidase D, an antioxidant protein in mycobacterium (Ho et al. 2016). Under genotoxic damage or oxidative stress, adaptive sestrin2 expression in a p53-dependent manner prevents reactive oxygen species-induced cytotoxicity and cell death (Lee et al. 2013). Specifically, Nrf2 and the

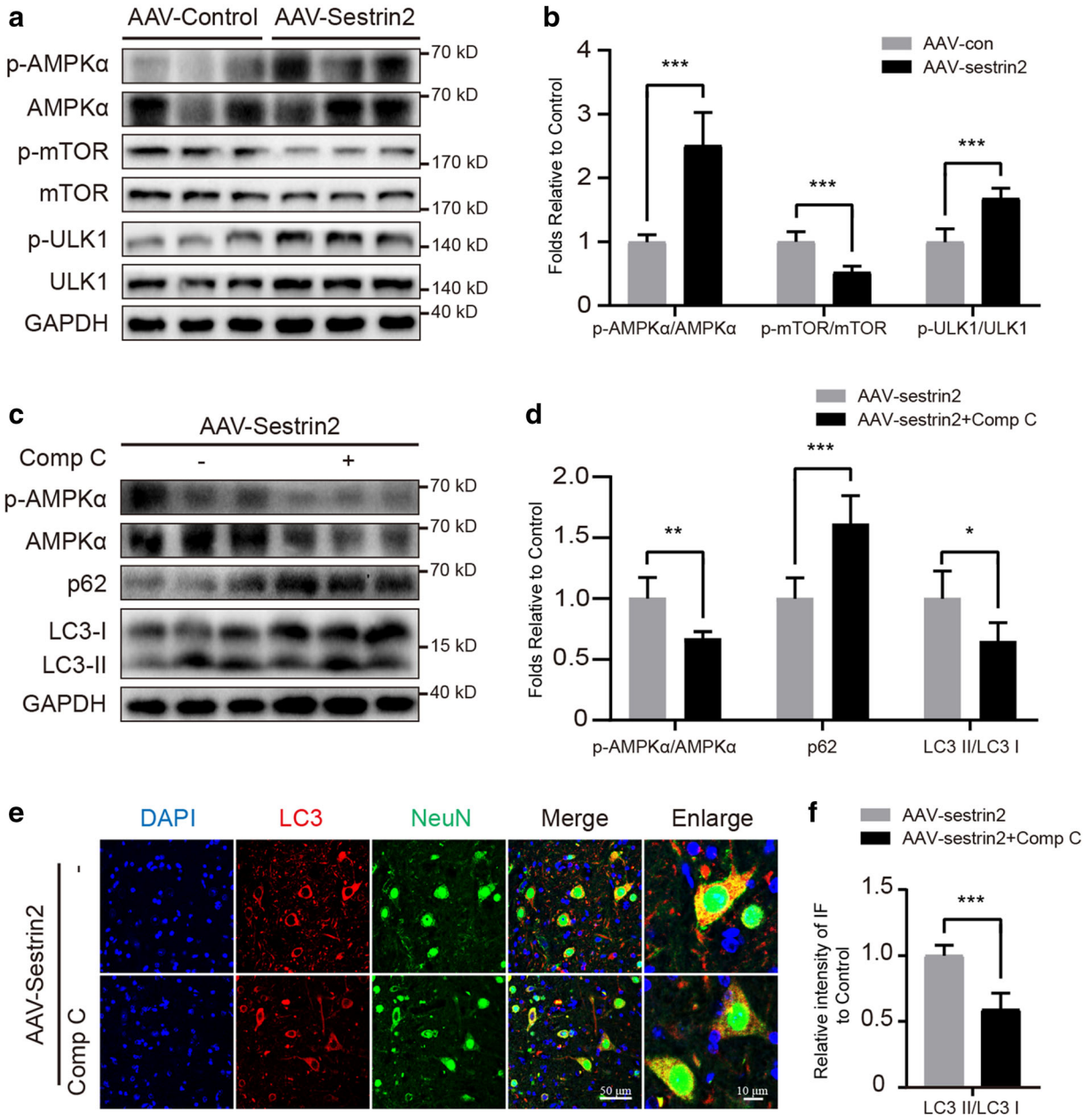

Fig. 8 AMPK-mTOR axis is responsible for sestrin2 induced autophagy. (**a** and **b**) Western blot and quantification of phosphorylation and total of AMPK, mTOR and ULK1 mice injected with AAV-control or AAV-sestrin2 for 14 days. (**c** and **d**) Western blot and quantification of phosphorylation and total of AMPK, p62, and LC3 in mice treated with Compound C (10 mg/kg) or saline that parallels with AAV injection. (**e** and **f**) Double staining of LC3 and NeuN in each group as above, scale bar = 50 μm; scale bar (enlarged) = 10 μm. GAPDH was the loading control. Data represent mean ± S.D. (n = 6). $^{*}P < 0.05$, $^{**}P < 0.01$, $^{***}P < 0.001$

antioxidant response element response axis are also required for the upregulation of sestrin2 (Shin et al. 2012). As a matter of fact, sestrin2 has another name, hypoxia inducible gene 95, and was originally discovered in cells under hypoxia environment. The mechanism of sestrin2 induction in response to hypoxia mainly depends on HIF-1 activation. Moreover, as the consequence of energy deprivation secondary to continued hypoxia, sestrin2 could be induced in a HIF-1-independent mechanism (Lee et al. 2013).

ER stress and UPR are common and crucial molecular events in neural trauma. To the best of our

knowledge, the regulation of sestrin2 in neurons upon ER stress has not been thoroughly explicated. Park et al. (2014) indicated that ER stress induced by palmitic acid could activate sestrin2 expression in hepatocytes. In the current study, we found that there was a significant increase in sestrin2 expression in spinal cord after injury and primary neuron treatment with TM in vitro. Moreover, it has been well characterized that UPR is an adaptive process activated by ER sensors and leads cells to induce numerous transcriptional processes in the face of impaired proteostasis. Ye et al. (2015) reported that the upregulation of ATF4 induces expression of the stress response protein sestrin2 during amino acid deprivation. Moreover, Park et al. (2014) suggested that PERK and c/EBPβ are responsible for the expression of sestrin2 in response to ER stress in hepatocytes. Consistent with previous studies, the results of this study indicated that the activation of PERK and ATF4 is involved in sestrin2 induction under ER stress in neurons after SCI.

Previous studies demonstrated that restoring ER function is one of the available strategies for acute neural injury, as it helps neurons against ER stress induced apoptosis (Wan et al. 2019; Zhao et al. 2016). In the present study, we also identified that upregulation of sestrin2 by AAV provides beneficial effects in reducing ER stress and apoptosis. However, the mechanism regarding sestrin2 contribution to ER homeostasis has not been well identified. As previously reported, sestrin2 can enhance autophagy during diverse environmental stresses, which is responsible for the clearance of damaged mitochondria, attenuating insulin resistance (Kim et al. 2016; Li et al. 2017). Here, we hypothesized that the lessened ER stress by sestrin2 overexpression is associated with activation of autophagy after SCI.

Subsequently, we assessed the status of autophagy and the link between sestrin2 and autophagy in neurons. In the current study, the ratio of LC3-II/I appeared increased, which be the result of dysfunction of lysosomes or failed autolysosome formation. A previous study mentioned that autophagosomes are activated in spinal cord after acute traumatic injury (Sarkar et al. 2014). However, accumulating evidence has indicated that lysosomes are impaired and cannot effectively combine with autophagosomes when neurons undergo alterations of the intracellular and the extracellular microenvironment in neural injury (Cai et al. 2016; Liu et al. 2015). The inhibited autophagic flux leads to exacerbation of ER stress, as autophagy is one of the processes initiated for the elimination of misfolded proteins. The present study showed that the restoration of autophagic flux mediated by sestrin2 overexpression contributes to alleviation of ER stress and apoptosis.

The results presented here showed that the mechanism of increased autophagy in the spinal cord of AAV-sestrin2 mice is a result of the significant regulation of the AMPK-mTOR axis, as evidenced by treatment with AMPK inhibitor. As a functional regulator in maintaining cell survival and homeostasis, AMPK phosphorylation is modulated by sestrin2 induction, which has been previously identified. The mechanism by which sestrin2 regulates AMPK involves sestrin2 binding to AMPK and forming a complex, increasing AMPK phosphorylation at Thr172 (Quan et al. 2017). Moreover, sestrin2-mediated AMPK activity has been shown to be important for inhibition of mTOR and phosphorylation of ULK1, which has been proposed to be a crucial positive regulator for autophagy induction (Ho et al. 2016). Moreover, the amelioration of lysosomal function is essential for autophagic flux restoration. Previous studies indicated that the lysosome is the signaling hub of mTOR regulation and mTOR regulates lysosomal function through modulating the localization of TFEB, which is a major factor for regulating lysosomal protein activity and lysosomal biogenesis (Civiletto et al. 2018). We regarded mTOR as the main regulator in modulating Lamp2 and CTSB, two lysosomal markers, though there is no definite mechanism revealing the effect of sestrin2 on lysosomal function.

Certainly, there are several limitations regarding the use of sestrin2 as a therapy target for SCI, and the underlying molecular mechanism still requires further study and investigation. For instance, in view of the complexity of and various cell structures found in the spinal cord, primary cortical neurons cultured alone in vitro are informative. In the current study, we also found that the change in sestrin2 expression was not only present in neurons but also other cells. Therefore, the focus on the effect of sestrin2 on neurons may be one-sided in the current study. Additionally, we note that employing plasmid or gene knockdown instead of molecular inhibitors would be more persuasive. Nevertheless, the effect of sestrin2 on functional recovery after SCI is

confirmed, and the properties and underlying mechanisms can be clarified in future studies.

In summary, the current study demonstrated that the regulation of sestrin2 is a stress-inducible process in the adaptive response to SCI and pharmacological ER stress that was mainly activated by the PERK-ATF4 axis of the UPR. Moreover, the results of our study also suggested that sestrin2 promotes functional recovery and neuronal survival after SCI through attenuation of ER stress that is mediated by the activation of autophagy and restoration of autophagic flux as a consequence of AMPK-mTOR axis regulation. Therefore, the above evidence suggests that sestrin2 could exhibit neuroprotection and appears to be a feasible therapeutic target for acute traumatic SCI.

Author contributions Yao Li designed the research and wrote the paper; Jing Zhang and Kailiang Zhou assisted in performing the in vivo and in vitro experiments; Ling Xie, Guangheng Xiang, and Mingqiao Fang guided the experiments and image acquisition; Wen Han modified the syntax of the paper; Xiangyang Wang and Xiao Jian assisted in designing the research and approved the final version to be submitted.

Funding information This work was supported by grants from Natural Science Foundation of China (81722028, 81972150), Zhejiang Public Service Technology Research Program and Social Development (LGF18H060008), Natural Science Foundation of Zhejiang.

Province (LR18H50001, LQ18H090008), CAMS Innovation Fund for Medical Sciences (2019-I2M-5-028).

Compliance with ethical standards

Conflict of interest The authors declare no conflicts of interest.

References

Araki K, Nagata K. Protein folding and quality control in the ER. Cold Spring Harb Perspect Biol. 2011;3(11):a007526. https://doi.org/10.1101/cshperspect.a007526.

Badhiwala JH, Wilson JR, Fehlings MG. Global burden of traumatic brain and spinal cord injury. Lancet Neurol. 2019;18(1):24–5. https://doi.org/10.1016/S1474-4422(18)30444-7.

Basso DM, Fisher LC, Anderson AJ, Jakeman LB, McTigue DM, Popovich PG. Basso mouse scale for locomotion detects differences in recovery after spinal cord injury in five common mouse strains. J Neurotrauma. 2006;23(5):635–59. https://doi.org/10.1089/neu.2006.23.635.

Borgese N, Francolini M, Snapp E. Endoplasmic reticulum architecture: structures in flux. Curr Opin Cell Biol. 2006;18(4):358–64. https://doi.org/10.1016/j.ceb.2006.06.008.

Budanov AV, Shoshani T, Faerman A, Zelin E, Kamer I, Kalinski H, et al. Identification of a novel stress-responsive gene Hi95 involved in regulation of cell viability. Oncogene. 2002;21(39):6017–31. https://doi.org/10.1038/sj.onc.1205877.

Cai Y, Arikkath J, Yang L, Guo ML, Periyasamy P, Buch S. Interplay of endoplasmic reticulum stress and autophagy in neurodegenerative disorders. Autophagy. 2016;12(2):225–44. https://doi.org/10.1080/15548627.2015.1121360.

Chen YS, Chen SD, Wu CL, Huang SS, Yang DI. Induction of sestrin2 as an endogenous protective mechanism against amyloid beta-peptide neurotoxicity in primary cortical culture. Exp Neurol. 2014;253:63–71. https://doi.org/10.1016/j.expneurol.2013.12.009.

Civiletto G, Dogan SA, Cerutti R, Fagiolari G, Moggio M, Lamperti C, et al. Rapamycin rescues mitochondrial myopathy via coordinated activation of autophagy and lysosomal biogenesis. EMBO Mol Med. 2018;10(11). https://doi.org/10.15252/emmm.201708799.

Courtine G, Sofroniew MV. Spinal cord repair: advances in biology and technology. Nat Med. 2019;25(6):898–908. https://doi.org/10.1038/s41591-019-0475-6.

Doeppner TR, Kaltwasser B, Bahr M, Hermann DM. Effects of neural progenitor cells on post-stroke neurological impairment-a detailed and comprehensive analysis of behavioral tests. Front Cell Neurosci. 2014;8:338. https://doi.org/10.3389/fncel.2014.00338.

Engel T, Sanz-Rodgriguez A, Jimenez-Mateos EM, Concannon CG, Jimenez-Pacheco A, Moran C, et al. CHOP regulates the p53-MDM2 axis and is required for neuronal survival after seizures. Brain. 2013;136(Pt 2):577–92. https://doi.org/10.1093/brain/aws337.

Han J, Back SH, Hur J, Lin YH, Gildersleeve R, Shan J, et al. ER-stress-induced transcriptional regulation increases protein synthesis leading to cell death. Nat Cell Biol. 2013;15(5):481–90. https://doi.org/10.1038/ncb2738.

Ho A, Cho CS, Namkoong S, Cho US, Lee JH. Biochemical basis of Sestrin physiological activities. Trends Biochem Sci. 2016;41(7):621–32. https://doi.org/10.1016/j.tibs.2016.04.005.

Kim MJ, Bae SH, Ryu JC, Kwon Y, Oh JH, Kwon J, et al. SESN2/sestrin2 suppresses sepsis by inducing mitophagy and inhibiting NLRP3 activation in macrophages. Autophagy. 2016;12(8):1272–91. https://doi.org/10.1080/15548627.2016.1183081.

Lee JH, Budanov AV, Park EJ, Birse R, Kim TE, Perkins GA, et al. Sestrin as a feedback inhibitor of TOR that prevents age-related pathologies. Science. 2010;327(5970):1223–8. https://doi.org/10.1126/science.1182228.

Lee JH, Budanov AV, Karin M. Sestrins orchestrate cellular metabolism to attenuate aging. Cell Metab. 2013;18(6):792–801. https://doi.org/10.1016/j.cmet.2013.08.018.

Li L, Xiao L, Hou Y, He Q, Zhu J, Li Y, et al. Sestrin2 silencing exacerbates cerebral ischemia/reperfusion injury by decreasing mitochondrial biogenesis through the AMPK/PGC-1alpha pathway in rats. Sci Rep. 2016;6:30272. https://doi.org/10.1038/srep30272.

Li H, Liu S, Yuan H, Niu Y, Fu L. Sestrin 2 induces autophagy and attenuates insulin resistance by regulating AMPK signaling in C2C12 myotubes. Exp Cell Res. 2017;354(1):18–24. https://doi.org/10.1016/j.yexcr.2017.03.023.

Li Y, Han W, Wu Y, Zhou K, Zheng Z, Wang H, et al. Stabilization of hypoxia inducible factor-1alpha by Dimethyloxalylglycine promotes recovery from acute spinal cord injury by inhibiting neural apoptosis and enhancing axon regeneration. J Neurotrauma. 2019;36(24):3394–409. https://doi.org/10.1089/neu.2018.6364.

Liu S, Sarkar C, Dinizo M, Faden AI, Koh EY, Lipinski MM, et al. Disrupted autophagy after spinal cord injury is associated with ER stress and neuronal cell death. Cell Death Dis. 2015;6:e1582. https://doi.org/10.1038/cddis.2014.527.

Morris G, Puri BK, Walder K, Berk M, Stubbs B, Maes M, et al. The endoplasmic reticulum stress response in neuroprogressive diseases: emerging pathophysiological role and translational implications. Mol Neurobiol. 2018;55(12):8765–87. https://doi.org/10.1007/s12035-018-1028-6.

Morrison A, Chen L, Wang J, Zhang M, Yang H, Ma Y, et al. Sestrin2 promotes LKB1-mediated AMPK activation in the ischemic heart. FASEB J. 2015;29(2):408–17. https://doi.org/10.1096/fj.14-258814.

Nakka VP, Prakash-Babu P, Vemuganti R. Crosstalk between endoplasmic reticulum stress, oxidative stress, and autophagy: potential therapeutic targets for acute CNS injuries. Mol Neurobiol. 2016;53(1):532–44. https://doi.org/10.1007/s12035-014-9029-6.

Ohtake Y, Sami A, Jiang X, Horiuchi M, Slattery K, Ma L, et al. Promoting axon regeneration in adult CNS by targeting liver kinase B1. Mol Ther. 2019;27(1):102–17. https://doi.org/10.1016/j.ymthe.2018.10.019.

Olson N, Hristova M, Heintz NH, Lounsbury KM, van der Vliet A. Activation of hypoxia-inducible factor-1 protects airway epithelium against oxidant-induced barrier dysfunction. Am J Physiol Lung Cell Mol Physiol. 2011;301(6):L993–L1002. https://doi.org/10.1152/ajplung.00250.2011.

Parikh P, Hao Y, Hosseinkhani M, Patil SB, Huntley GW, Tessier-Lavigne M, et al. Regeneration of axons in injured spinal cord by activation of bone morphogenetic protein/Smad1 signaling pathway in adult neurons. Proc Natl Acad Sci U S A. 2011;108(19):E99–107. https://doi.org/10.1073/pnas.1100426108.

Park HW, Park H, Ro SH, Jang I, Semple IA, Kim DN, et al. Hepatoprotective role of Sestrin2 against chronic ER stress. Nat Commun. 2014;5:4233. https://doi.org/10.1038/ncomms5233.

Pasha M, Eid AH, Eid AA, Gorin Y, Munusamy S. Sestrin2 as a novel biomarker and therapeutic target for various diseases. Oxidative Med Cell Longev. 2017;2017:3296294–10. https://doi.org/10.1155/2017/3296294.

Quan N, Sun W, Wang L, Chen X, Bogan JS, Zhou X, et al. Sestrin2 prevents age-related intolerance to ischemia and reperfusion injury by modulating substrate metabolism. FASEB J. 2017;31(9):4153–67. https://doi.org/10.1096/fj.201700063R.

Salvany S, Casanovas A, Tarabal O, Piedrafita L, Hernandez S, Santafe M, et al. Localization and dynamic changes of neuregulin-1 at C-type synaptic boutons in association with motor neuron injury and repair. FASEB J. 2019;33(7):7833–51. https://doi.org/10.1096/fj.201802329R.

Sarkar C, Zhao Z, Aungst S, Sabirzhanov B, Faden AI, Lipinski MM. Impaired autophagy flux is associated with neuronal cell death after traumatic brain injury. Autophagy. 2014;10(12):2208–22. https://doi.org/10.4161/15548627.2014.981787.

Shi X, Doycheva DM, Xu L, Tang J, Yan M, Zhang JH. Sestrin2 induced by hypoxia inducible factor1 alpha protects the blood-brain barrier via inhibiting VEGF after severe hypoxic-ischemic injury in neonatal rats. Neurobiol Dis. 2016;95:111–21. https://doi.org/10.1016/j.nbd.2016.07.016.

Shin BY, Jin SH, Cho IJ, Ki SH. Nrf2-ARE pathway regulates induction of Sestrin-2 expression. Free Radic Biol Med. 2012;53(4):834–41. https://doi.org/10.1016/j.freeradbiomed.2012.06.026.

Silva NA, Sousa N, Reis RL, Salgado AJ. From basics to clinical: a comprehensive review on spinal cord injury. Prog Neurobiol. 2014;114:25–57. https://doi.org/10.1016/j.pneurobio.2013.11.002.

Tator CH, Fehlings MG. Review of the secondary injury theory of acute spinal cord trauma with emphasis on vascular mechanisms. J Neurosurg. 1991;75(1):15–26. https://doi.org/10.3171/jns.1991.75.1.0015.

Valenzuela V, Collyer E, Armentano D, Parsons GB, Court FA, Hetz C. Activation of the unfolded protein response enhances motor recovery after spinal cord injury. Cell Death Dis. 2012;3:e272. https://doi.org/10.1038/cddis.2012.8.

Wan H, Wang Q, Chen X, Zeng Q, Shao Y, Fang H, et al. WDR45 contributes to neurodegeneration through regulation of ER homeostasis and neuronal death. Autophagy. 2019;16:1–17. https://doi.org/10.1080/15548627.2019.1630224.

Wang Q, Zhang H, Xu H, Zhao Y, Li Z, Li J, et al. Novel multi-drug delivery hydrogel using scar-homing liposomes improves spinal cord injury repair. Theranostics. 2018a;8(16):4429–46. https://doi.org/10.7150/thno.26717.

Wang Y, Wu W, Wu X, Sun Y, Zhang YP, Deng LX, et al. Remodeling of lumbar motor circuitry remote to a thoracic spinal cord injury promotes locomotor recovery. eLife. 2018b;7. https://doi.org/10.7554/eLife.39016.

Wang P, Zhao Y, Li Y, Wu J, Yu S, Zhu J, et al. Sestrin2 overexpression attenuates focal cerebral ischemic injury in rat by increasing Nrf2/HO-1 pathway-mediated angiogenesis. Neuroscience. 2019;410:140–9. https://doi.org/10.1016/j.neuroscience.2019.05.005.

Ye J, Palm W, Peng M, King B, Lindsten T, Li MO, et al. GCN2 sustains mTORC1 suppression upon amino acid deprivation by inducing Sestrin2. Genes Dev. 2015;29(22):2331–6. https://doi.org/10.1101/gad.269324.115.

Yin Y, Sun G, Li E, Kiselyov K, Sun D. ER stress and impaired autophagy flux in neuronal degeneration and brain injury. Ageing Res Rev. 2017;34:3–14. https://doi.org/10.1016/j.arr.2016.08.008.

Yu PB, Hong CC, Sachidanandan C, Babitt JL, Deng DY, Hoyng SA, et al. Dorsomorphin inhibits BMP signals required for embryogenesis and iron metabolism. Nat Chem Biol. 2008;4(1):33–41. https://doi.org/10.1038/nchembio.2007.54.

Zhang D, Xuan J, Zheng BB, Zhou YL, Lin Y, Wu YS, et al. Metformin improves functional recovery after spinal cord injury via autophagy flux stimulation. Mol Neurobiol. 2017;54(5):3327–41. https://doi.org/10.1007/s12035-016-9895-1.

Zhao YZ, Jiang X, Xiao J, Lin Q, Yu WZ, Tian FR, et al. Using NGF heparin-poloxamer thermosensitive hydrogels to enhance the nerve regeneration for spinal cord injury. Acta Biomater. 2016;29:71–80. https://doi.org/10.1016/j.actbio.2015.10.014.

Zheng Z, Zhou Y, Ye L, Lu Q, Zhang K, Zhang J, et al. Histone deacetylase 6 inhibition restores autophagic flux to promote functional recovery after spinal cord injury. Exp Neurol. 2019;324:113138. https://doi.org/10.1016/j.expneurol.2019.113138.